

## Observation and measurement of internucleotide ${}^2J_{\text{NN}}$ coupling constants between ${}^{15}\text{N}$ nuclei with widely separated chemical shifts

Ananya Majumdar\*, Abdelali Kettani & Eugene Skripkin

*Cellular Biochemistry and Biophysics Program, Memorial Sloan-Kettering Cancer Center, 1275 York Avenue, New York, NY 10021, U.S.A.*

Received 7 December 1998; Accepted 28 January 1999

*Key words:* HNN-COSY, internucleotide  ${}^{15}\text{N}$  couplings,  ${}^2J_{\text{NN}}$ , spin-echo difference

### Abstract

Scalar coupling correlations between hydrogen bonded  ${}^{15}\text{N}$  nuclei in non Watson–Crick base pairs is a critical step in the structure determination of unusual nucleic acids. For observing the  ${}^2J_{\text{NN}}$  coupling constant between far upfield N2,N6 (amino) nitrogens and far downfield (N1,N3,N7) nitrogens (separated by 150–160 ppm), the HNN-COSY experiment (Dingley and Grzesiek, 1998) is rather insensitive, due to technical difficulties associated with simultaneous excitation of both extremes of the  ${}^{15}\text{N}$  spectrum. These nuclei may be correlated by treating them in a pseudo-heteronuclear manner, using  ${}^{15}\text{N}$  selective pulses. The wide chemical shift separation allows accurate measurement of the  ${}^2J_{\text{NN}}$  coupling constant using spin-echo difference methods. Pulse sequences for observation and measurement of  ${}^2J_{\text{NN}}$  coupling constants between amino and N7 nuclei are presented and demonstrated on an A-A mismatch segment of the uniformly ( ${}^{15}\text{N}$ ,  ${}^{13}\text{C}$ ) labelled DNA sample, d(GGAGGAT)<sub>2</sub>.

Recently, Dingley and Grzesiek (1998) and Pervushin et al. (1998) have reported the observation of  ${}^2J_{\text{NN}}$  coupling constants between hydrogen bonded base pairs in  ${}^{15}\text{N}$  labelled RNA. They have observed and measured the homonuclear  ${}^2J_{\text{NN}}$  coupling between N3 (U), N1 (G) donors and N1 (A), N3 (C) acceptors, base paired in Watson–Crick fashion. These remarkable observations assume a vital role in structure elucidation of nucleic acids, especially those involving non Watson–Crick hydrogen bonding schemes (Neidle, 1995; Patel et al., 1998). Often, these base-pairing schemes are proposed on the basis of indirect observations such as NOEs involving the hydrogen bonded protons, their solvent exchange rates and their chemical shifts. The unambiguous evidence provided by direct observation of scalar couplings between hydrogen bonded  ${}^{15}\text{N}$  donors and acceptors vastly improves the quality and accuracy of the final structure.

The  ${}^2J_{\text{NN}}$ -HNN-COSY sequence of Dingley and Grzesiek is well suited for obtaining N-N correlations

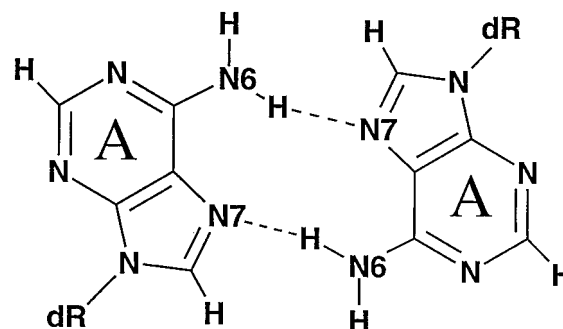
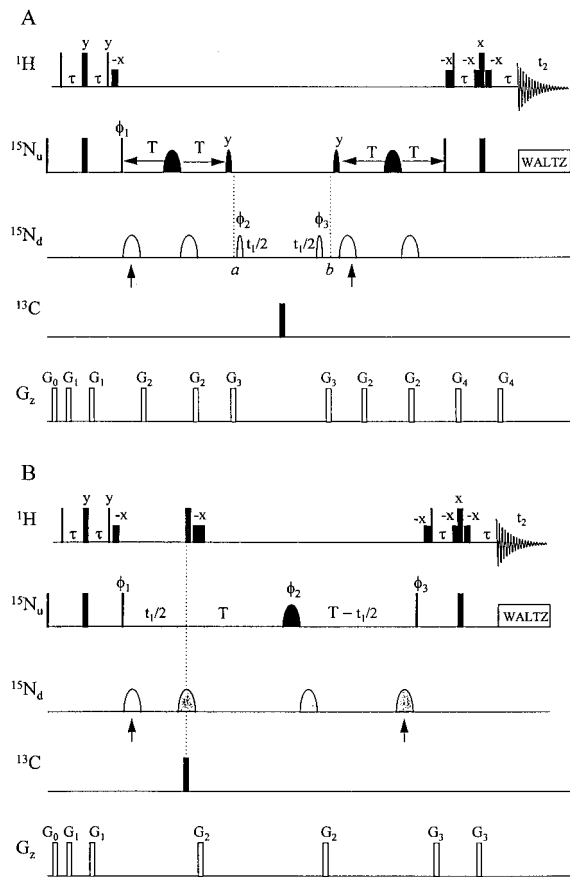


*Figure 1.* Schematic of the A-A mismatch proposed for the structure of the d(GGAGGAT)<sub>2</sub> sequence, indicating hydrogen bonds between N6 (amino) and N7 nitrogens.

involving imino ( $N_i$ ) nitrogens (N1 of G and N3 of U/T), whose chemical shifts ( $\sim 150$  ppm) are nearly midway between the most upfield amino ( $N_a$ ) nitrogens (N2 of G and N6 of A,  $\sim 80$  ppm) and the most downfield aromatic ( $N_d$ ) nitrogens (N7 of A, G and N1,N3 of A, 210–240 ppm). The separation between the imino nitrogens and either extreme of the  ${}^{15}\text{N}$  spectrum is small enough (5–6 kHz, at 600 MHz

\*To whom correspondence should be addressed. E-mail: majumdar@sbnmr1.ski.mskcc.org



$^1\text{H}$  frequency) to permit correlations between them in a straightforward, homonuclear manner. The sequence can therefore be applied to observation of  $^2J_{\text{NN}}$  couplings involving  $\text{N}_i\text{-N}_a$  or  $\text{N}_i\text{-N}_d$  mismatched base pairs. In our laboratory, we have successfully applied the method to observe several such correlations in G-G and A-A mismatches in a novel, arrowhead motif adopted by the DNA sequence  $\text{d}(\text{GGAGGAT})_2$  (Kettani et al., 1998). Serious technical difficulties arise, however, when attempting  $\text{N}_a\text{-N}_d$  correlations, where the chemical shift differences lie in the range of 9–10 kHz at 600 MHz ( $^1\text{H}$ ). With present day technology, available rf field strengths for  $^{15}\text{N}$  (6–8 kHz) are extremely inefficient for simultaneous excitation of  $\text{N}_a$  (N2,N6) and  $\text{N}_d$  (N1,N3,N7) nitrogens. This is particularly true for  $180^\circ$  pulses, which are critical for developing the  $^2J_{\text{NN}}$  coupling. For such situations, the solution lies in treating the upfield and downfield nitrogens as pseudo heteronuclei and manipulating them separately using selective nitrogen pulses. The relatively large  $\text{N}_a\text{-N}_d$  separation turns out to be an ad-

Figure 2. (A) The s-HNN-COSY pulse sequence for correlating upfield ( $\text{N}_u$ ) and downfield ( $\text{N}_d$ ) hydrogen bonded nitrogens. Narrow and wide pulses (both square as well as shaped) represent  $90^\circ$  and  $180^\circ$  pulses, respectively, with phase  $x$ , unless indicated otherwise. The  $^1\text{H}$  and  $^{13}\text{C}$  carriers were placed at 5.0 ppm (water) and 160 ppm, respectively. The  $^{15}\text{N}$  carrier was placed in the center of the  $\text{N}_u$  region (80 ppm) until point  $a$  in the sequence, when it was switched to the center of the  $\text{N}_d$  region (226 ppm), and then switched back to 80 ppm at point  $b$ . Rf field strengths employed were:  $^1\text{H}$ : hard pulses: 39 kHz, square pulses (for water flip-back (Grzesiek and Bax, 1993; Kuboniwa et al., 1994) and WATERGATE (Piotto et al., 1992)): 0.125 kHz (2.0 ms);  $^{13}\text{C}$ : 20 kHz;  $^{15}\text{N}$ : hard pulses: 5.6 kHz, WALTZ (Shaka et al., 1983) decoupling during acquisition ( $t_2$ ): 1.2 kHz, selective refocusing pulses (filled): 0.62 ms (4.2 kHz peak rf) rsnob pulses (Kupce et al., 1995), selective inversion pulses (open), phase-modulated at 146 ppm (Boyd and Scoffe, 1989; Patt, 1992): 0.92 ms iburp1 pulses (Geen and Freeman, 1991) (3.7 kHz peak rf), selective  $M_z \rightarrow M_{xy}$   $90^\circ$  pulses (filled): 1.5 ms qsneeze pulses (Kupce and Freeman, 1995) (3.3 kHz peak rf), selective  $M_{xy} \rightarrow M_z$   $90^\circ$  pulses (filled): 1.5 ms time-reversed qsneeze pulses. The shaped pulse durations were optimized for 600 MHz ( $^1\text{H}$ ). Pulses marked with an arrow are applied for Bloch-Siegert shift compensation (Vuister and Bax, 1992). Delays used were:  $\tau = 2.4$  ms,  $T = 22$  ms. Phase cycles:  $\phi_1 = x, -x$ ,  $\phi_2 = 2(x), 2(-x)$ ,  $\phi_3 = 4(x), 4(-x)$ , Receiver =  $x, -x, -x, x, -x, x, x, -x$ . Quadrature detection in the  $\omega_1$  dimension was achieved by States-TPPI phase cycling (Marion et al., 1989) of  $\phi_2$ . Gradients (G/cm)/durations (ms):  $G_0 = 32/2.0$ ,  $G_1 = 16/0.5$ ,  $G_2 = 24/1.0$ ,  $G_3 = 30/1.0$ ,  $G_4 = 30/1.0$ ,  $G_5 = 30/0.35$ . (B) Pulse sequence for measuring  $^2J_{\text{NNd}}$  couplings using the spin-echo difference method. All pulse/rf related parameters are identical to the sequence in Figure A with the following differences: The  $^{15}\text{N}$  carrier was set at 80 ppm throughout the sequence. The selective inversion pulse was phase-modulated at 165 ppm so as to be centered on the downfield edge of  $\text{N}_d$  (245 ppm), and was of duration 3.0 ms (1.3 kHz, peak rf) to avoid excitation of the intranucleotide N1 nitrogen. The positions of the open and filled  $\text{N}_d$  inversion pulses correspond to the experiments where the  $^2J_{\text{NNd}}$  is active and inactive, respectively. Pulses for Bloch-Siegert compensation are marked with arrows. The water magnetization was returned to the  $+z$  axis with a water-selective  $180^\circ$  pulse immediately after the  $^1\text{H}$  decoupling pulse. The delay  $T$  was varied from 30–60 ms (see Figure 4). Phase cycles:  $\phi_1 = (x, -x) + \text{States-TPPI}$ ,  $\phi_2 = 2(x), 2(y), 2(-x), 2(-y)$ ;  $\phi_3 = 8(x), 8(-x)$ ; Receiver = ABBA, A =  $x, -x, -x, x$ , B =  $-x, x, x, -x$ . Gradients (G/cm)/Durations (ms):  $G_0 = 32/2.0$ ,  $G_1 = 16/1.0$ ,  $G_2 = 30/1.0$ ,  $G_3 = 15/0.3$ .

vantage when measuring the  $^2J_{\text{NN}}$  coupling constant, because the spin-echo difference method developed by Bax and co-workers (Bax et al., 1994) may be used effectively.

In this communication, we present pulse sequences for the observation and measurement of  $^2J_{\text{NN}}$  couplings between upfield ( $\text{N}_u = \text{N}_a, \text{N}_i$ ) donors and far downfield ( $\text{N}_d$ ) acceptors. Specifically for the purpose of this communication, we discuss the  $^2J_{\text{NN}}$  coupling between hydrogen bonded A3 amino (N6) and A6 (N7), and A6 amino (N6) and A3 (N7) nitrogens in the sequence  $\text{d}(\text{GGAGGAT})_2$  (Figure 1).

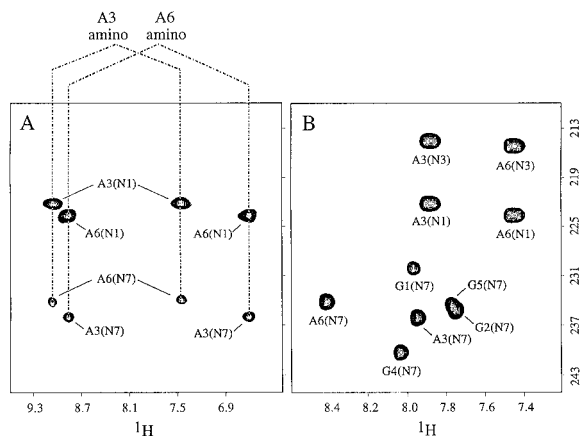
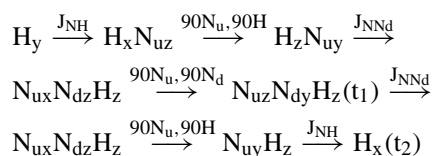


**Figure 3.** (A) Spectrum showing internucleotide N6-N7 and intranucleotide N6-N1 cross peaks of the A3-A6 base pair, recorded using the *s*-HNN-COSY sequence of Figure 2A, on a 0.3 mM sample of uniformly ( $^{15}\text{N}$ ,  $^{13}\text{C}$ ) labelled d(GGAGGAT) $_2$  at 0 °C. The spectrum was recorded on a Varian Inova spectrometer operating at 600 MHz ( $^1\text{H}$  frequency) and consisted of 864 ( $t_2$ ) and 44 ( $t_1$ ) complex data points with 400 transients/FID. Spectral widths of 2200 Hz ( $t_1^{\text{max}} = 20.0$  ms) and 12000 Hz ( $t_2^{\text{max}} = 72.0$  ms) were employed. Data were processed using Felix 97.0 (Molecular Simulations, Inc.). The final 2D matrix consisted of  $1024 (\omega_2) \times 128 (\omega_1)$  points. (B) Portion of a long range (H8,H2)-(N1,N3,N7) HSQC spectrum showing intraresidue assignments.

These hydrogen bonds were predicted from structure calculations based on NMR data (Kettani et al, 1998). On a 0.3 mM, uniformly ( $^{15}\text{N}$ ,  $^{13}\text{C}$ ) labelled sample at 0 °C, the HNN-COSY sequence was too insensitive to yield any data. The modified *s* (selective)-HNN-COSY pulse sequence used for obtaining the correlations is shown in Figure 2A. An outline of the magnetization transfer steps is as follows:



The final 2D spectrum contains cross peaks between the ( $\text{N}_{\text{u}}$ )H protons and the  $\text{N}_{\text{d}}$  nitrogens. Evolution of the  $\text{N}_{\text{uy}}\text{H}_z$  coherence under the  $^2J_{\text{NN}}$  coupling is achieved using selective refocussing pulses centered on  $\text{N}_{\text{u}}$  and linearly phase-modulated, selective inversion pulses centered on  $\text{N}_{\text{d}}$ . Coherence transfer  $\text{N}_{\text{ux}}\text{N}_{\text{dz}}\text{H}_z \rightarrow \text{N}_{\text{uz}}\text{N}_{\text{dy}}\text{H}_z$  is achieved through selective  $^{15}\text{N}$  90 °C pulses. During the  $t_1$  period,  $\text{N}_{\text{d}}$  may be selectively decoupled from  $\text{N}_{\text{u}}$  using frequency shifted inversion pulses centered on  $\text{N}_{\text{u}}$ , but may be omitted to minimize the number of selective pulses, especially if

the  $^2J_{\text{NN}}$  coupling constant is small. The TROSY unit (Pervushin et al., 1997) used in the final segment of the HNN-COSY sequence is not applicable to amino nitrogens, which have two attached protons. Additional sensitivity enhancement may be gained by replacing H-N INEPT steps with CPMG trains (Mueller et al., 1994). Figure 3A shows the internucleotide cross peaks between A3(N6)-A6(N7) and A6(N6)-A3(N7) and the intranucleotide N6-N1 cross peaks in the spectrum obtained using the *s*-HNN-COSY sequence. The relatively weak intensity of the A6:N6-A3:N7 cross peak is due to the broad amino proton resonance of A6, although the A3:N6-A6:N7 and A6:N6-A3:N7 coupling constants were found to be almost identical (see below). The N7 assignments were obtained from a long-range (H8,H2)-(N1,N3,N7) HSQC spectrum (Figure 3B). The intraresidue peaks were assigned to N1 rather than N3 based on the closer proximity of N1 to N6 (three bonds) than N3 (five bonds).

The pulse sequence for measuring the  $^2J_{\text{NN}}$  coupling constant using the spin-echo difference method is shown in Figure 2B. It is essentially the  $^{15}\text{N}$  analog of the technique developed for measuring  $J_{\text{CC}}$  coupling constants in proteins (Grzesiek et al., 1993). Two constant time HSQC spectra correlating  $\text{N}_{\text{u}}$  and its attached proton(s) are recorded, with the  $^2J_{\text{NN}}$  coupling being allowed to be active and inactive, respectively, during the constant time period 2T. This is achieved by altering the positions of the selective inversion pulses on  $\text{N}_{\text{d}}$  during the course of the sequence (Figure 2B). The ratio of cross peak intensities  $I_{\text{active}}/I_{\text{inactive}}$  ( $r(T)$ ) is equal to  $\cos(2\pi J_{\text{NNd}}T)$ , from which the coupling constant may be easily extracted. The advantage of this method is that relaxation effects are identical for both experiments and therefore, are eliminated upon taking the ratio. In this specific example, since N6 is coupled to both N1 and N7, care was taken to apply the selective pulse so as not to excite the N1 resonance, while applying the selective  $\text{N}_{\text{d}}$  pulse. This was verified from a long-range (H8,H2)- $\text{N}_{\text{d}}$  HSQC using the same selective pulse, in which no cross peaks from adenine H2 to N1/N3 were observed (data not shown). Data for the coupling constant measurement were collected as a function of the delay time T. Intensities of the two amino protons were averaged. The remarkably good fit of cross peak ratio  $r(T)$  to  $\cos(2\pi J_{\text{NN}}T)$  for the two cross peaks is shown in Figure 4 (A,B). The coupling constants  $^2J_{\text{NN}}$  (A3:N6-A6:N7) and  $^2J_{\text{NN}}$  (A6:N6-A3:N7) are obtained to be  $2.44 \pm 0.02$  and  $2.45 \pm 0.03$  Hz, respectively. These are small values relative to the  $\sim 7$  Hz observed by

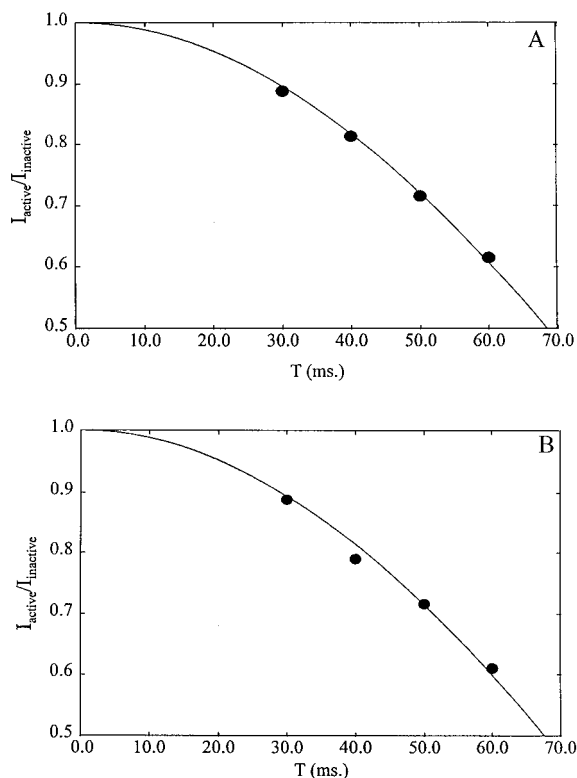


Figure 4. Plots of  $I_{\text{active}}/I_{\text{inactive}}$  vs.  $T$  (points) for A3:N6 (A) and A6:N6 (B), showing the fit to  $\cos(2\pi J_{\text{NN}}T)$  (line). Four data sets were acquired in an interleaved manner, with  $T = 30, 40, 50,$  and  $60$  ms. Each data set was acquired with  $864$  ( $t_2$ ) and  $32$  ( $t_1$ ) complex points, and  $160$  transients/FID. Spectral widths of  $1500$  Hz ( $\omega_1$ ,  $t_1^{\text{max}} = 21.3$  ms) and  $12000$  Hz ( $\omega_2$ ,  $t_2^{\text{max}} = 72.0$  ms) were employed. Data were processed using Felix 97.0 (Molecular Simulations, Inc.). The final 2D matrix for each data set consisted of  $1024$  ( $\omega_2$ )  $\times$   $128$  ( $\omega_1$ ) points.

Dingley and Grzesiek for Watson–Crick base pairs, which is possibly due to weaker hydrogen bonding in a mismatched alignment.

We have presented pulse sequences which effectively complement the HNN-COSY sequence of Dingley and Grzesiek for measuring  $^2J_{\text{NN}}$  coupling constants between hydrogen bonded  $^{15}\text{N}$  nuclei with widely disparate chemical shifts in nucleic acids. The sequences described here are not restricted to establishing amino (far upfield) to far downfield nitrogen correlations alone. Imino to downfield nitrogen correlations, especially for coupling constant measurement, may be obtained in the same way. The sequences are

likely to be even more useful on higher field spectrometers, where the chemical shift difference between the two extremes of the nitrogen spectrum is even greater.

### Acknowledgements

This research was supported under grant no. GM34504 to Dr. Dinshaw J. Patel. We thank D.J.P. for encouragement and discussions during the course of the work.

### References

- Bax, A., Vuister, G.W., Grzesiek, S., Delaglio, F., Wang, A.C., Tschudin, R. and Zhu, G. (1994) *Methods Enzymol.*, **239**, 79–105.
- Boyd, J. and Scoffe, N. (1989) *J. Magn. Reson.*, **85**, 406–413.
- Dingley, A.J. and Grzesiek, S. (1998) *J. Am. Chem. Soc.*, **120**, 8293–8297.
- Geen, H. and Freeman, R. (1991) *J. Magn. Reson.*, **93**, 93–141.
- Grzesiek, S., Vuister, G.W. and Bax, A. (1993) *J. Biomol. NMR*, **3**, 487–493.
- Grzesiek, S. and Bax, A. (1993) *J. Am. Chem. Soc.*, **115**, 3026–3027.
- Kettani, A., Bouaziz, S., Skripkin, E., Majumdar, A., Wang, W., Jones, R.A. and Patel, D.J., submitted for publication.
- Kuboniwa, H., Grzesiek, S., Delaglio, F. and Bax, A. (1994) *J. Biomol. NMR*, **4**, 871–878.
- Kupce, E., Boyd, J. and Campbell, I.D. (1995) *J. Magn. Reson.*, **B106**, 300–303.
- Kupce, E. and Freeman, R. (1995) *J. Magn. Reson.*, **A112**, 134–137.
- Marion, D., Ikura, M., Tschudin, R. and Bax, A. (1989) *J. Magn. Reson.*, **85**, 393–399.
- Mueller, L., Legault, P. and Pardi, A. (1995) *J. Am. Chem. Soc.*, **117**, 11043–11048.
- Neidle, S. (1995) *DNA Structure and Recognition*, Oxford University Press, Oxford.
- Patel, D.J., Bouaziz, S., Kettani, A. and Wang, Y. (1998) In *Oxford Handbook of Nucleic Acid Structures* (Ed., Neidle, S.), Oxford University Press, Oxford, pp. 389–453.
- Patt, S.L. (1992) *J. Magn. Reson.*, **96**, 94–102.
- Pervushin, K., Riek, R., Wider, G. and Wüthrich, K. (1997) *Proc. Natl. Acad. Sci. USA*, **94**, 12366–12371.
- Pervushin, K., Ono, A., Fernandez, C., Szyperski, T., Kainosho, M. and Wüthrich, K. (1998) *Proc. Natl. Acad. Sci. USA*, **95**, 14147–14151.
- Piotto, M., Saudek, V. and Sklenar, V. (1992) *J. Biomol. NMR*, **2**, 661–665.
- Shaka, A.J., Keeler, J., Frenkiel, T. and Freeman, R. (1983) *J. Magn. Reson.*, **52**, 335–338.
- Vuister, G.W. and Bax, A. (1992) *J. Magn. Reson.*, **98**, 428–435.